

Anfis Based wind Energy Conversion System For Power Quality Improvement In A Grid Tied Hybrid Generation System

D.Anitha¹, Dr. R.Kiranmayi² · Dr. P.Bharat Kumar³

¹ PG Student, Dept. of Electrical & Electronics Engineering, JNTUACEA, Anantapuramu, A.P India.515002

² Professor & Head Dept. of Electrical & Electronics Engineering, JNTUACEA, Anantapuramu, A.P India.515002

³ Lecturer, Dept. of Electrical & Electronics Engineering, JNTUACEA, Anantapuramu, A.P India.515002

Abstract:

This paper presents A failure mode and effect analysis is done for power converters and possible mitigation schemes are suggested for different faults. A 1:1 delta wye-grounded transformer is used at the inverter output to eliminate the triplet harmonics. Further, dynamic performances of both ANFIS with proportional-derivative and integral (PD+I) controller and classical proportional integral (PI) controller, to control the inverter currents extraction of optimum power and its dispatch by using Adaptive Neuro Fuzzy Interface Systems (ANFIS) from a grid tied hybrid generation system comprising of a permanent magnet synchronous generator based wind turbine and a low concentration photovoltaic generator. For photovoltaic generator, maximum power point tracking control is implemented using ANFIS under varying solar irradiance. Power extracted from wind turbine is designed as an ANFIS function of the dc link voltage error.

Keywords: MPPT, PMSG, ANFIS.

I. INTRODUCTION

Increased penetrations of renewable energy sources into the power grid arouse several challenges in integration not only amongst themselves but also between such sources and the grid. Though the energy obtained from such sources is environment friendly but the power and voltage obtained from such sources varies randomly with the variation of weather

This device maintains the power balance at the dc link which results in a smooth power dispatch. Li-ion batteries though costly have higher power density and can withstand higher charging/ discharging cycles than that of lead-acid batteries while NiMH batteries are costlier and have carcinogenic effect on the atmosphere in spite of having higher power density than Li-ion batteries. Low Concentration Photo Voltaic (LCPV) generator used in this work has a degree of

concentration of 2.2X which do not require any extra tracking mechanism and cooling arrangements for their cells. The use of such cells can increase solar power extraction efficiency to 20–25% than flat plate collectors, with the use of simple mirror reflection with good optical efficiency. In the proposed system maximum power extraction is essential from both LCPV generator and wind energy conversion system (WECS) for increasing system efficiency. ANFIS control has proved better than classical control for Maximum Power Point Tracking (MPPT) particularly under varying inputs for renewable energy sources. Tracking of maximum operating power point is done using source side variations which results in high frequency components in the dc link voltage. In this work optimum power is extracted from WECS using ANFIS algorithm based on the knowledge of direct (d) axis current error of the inverter (Δi_d), deviation in dc link voltage (ΔV_{dc}) with respect to its reference and its rate of change (δ (ΔV_{dc})). This technique performs well to stabilize dc link voltage and is devoid of high frequency components.

The crucial challenge is fast damping of oscillations in dc link voltage during rapid changes in wind speed under wind turbulence and change in solar irradiance while dispatching the extracted power, at the PCC. Furthermore, sag ride through of the inverter voltage would not be possible if the inverter reactive power compensation for load variation is inappropriate. The earlier papers cited do not focus keenly into these aspects altogether. The BESS control aims to regulate the dc link voltage (V_{dc}) as for a grid connected system fast power transfer at the PCC is possible if V_{dc} remains constant under all circumstances. Voltage Oriented Control (VOC) of a two-level fully controlled inverter is done as the load system considered requires no neutral grounding and switching losses may be reduced unlike higher-level inverters. The VOC is designed to achieve an improved quality power to be fed at the grid, apart from load reactive power compensation for power factor improvement and

voltage stabilization at the load bus [16]. Low pass filtered references for both active and reactive current components are used to reduce power distortions at the PCC. This method along with the passive L-C-L filter at the inverter output together improves both voltage and current THD.

A Failure Mode and Effect Analysis (FMEA) of the power conditioning interface between the generators and the grid is also discussed. Possible mitigation methods for system protection for faults in different converters are shown. This analysis is of importance in such hybrid system as the continuous heating of the power switches; improper heat sink and ageing may result in either open or short circuit faults in converters switches, failures in line inductors and capacitors. This hampers power conversion process, degrades power quality and incurs economic losses..

II. SYSTEM CONFIGURATION

a Permanent Magnet Synchronous Generator (PMSG) based WECS-LCPV hybrid system with Li-ion battery storage is considered. The proposed system is feeding power to a local load and the grid

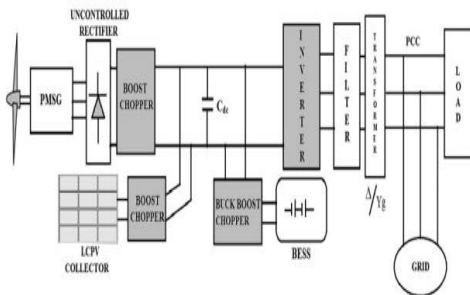


Fig. 1. System Configuration of a PMSG based WECS and LCPV connected to a power grid.

Table 1 Variable load switching schedule

Load	Value (P+jQ)	Switching scheme
L ₁	P=113 KW, Q=0.5 KVAR	Always remain connexed
L ₂	P=5 KW, Q=0.5 KVAR	From time =2 s to time =3 s
L ₃	P=15 KW, Q=0.75 KVAR	From time =3.5 s to time =4 s
L ₄	P=7 KW, Q=0.3 KVAR	From time =0 s to time =1.5 s and From time =3.5 s to time =4 s

A. LCPV system

LCPV generators are emerging as better choice over flat plate photovoltaic generators as the solar concentration can be enhanced to more than 6X with no tracking and extra cooling arrangement thus enabling power extraction at a higher efficiency. Basic one diode equivalent circuit is used in this work, where solar concentration of 2.2X is assumed to vary due to cloud intervention. The solar irradiance is in per unit (pu), (G_{pu}) over its base value of 1 KW/ m² . The ambient temperature and the cell temperature T_c [°C] are dependent on G_{pu} as per (1) and (2), as both temperature and irradiance regulates the output extractable power from the LCPV collector. An increase in cell temperature decreases the amount of possible power extraction unlike an increase in solar irradiance

$$T_a = 22 + 0.05(G_{pu} - 1.2) \tag{1}$$

$$T_c = T_a + \frac{G(T_c^{nom} - T_a^{nom})}{G_{nom}} \tag{2}$$

Wind Energy Conversion System:

A one mass drive train for PMSG-turbine shaft model is chosen in this work. While the generator rated speed is low, the speed difference between the turbine and the generator is considered negligible thus almost neglecting the contribution of viscous friction. The mechanical torque generated is given in (3), while the PMSG voltage and torque dynamics are represented in the direct-quadrature (d-q) axes from rotor reference frame of the PMSG.

$$T_m = \frac{1}{w_r} \{0.5pAC_p(\lambda, \beta)V_w^3\} \tag{3}$$

$$V_d = (r_s + L_d p)i_d - E_d \tag{4}$$

$$V_q = (r_s + L_q p) i_q - E_q \quad (5)$$

$$E_d = w_r L_q i_q \quad (6)$$

$$E_q = w_r L_d i_d + w_r \phi_r \quad (7)$$

$$T_c = \frac{3}{2} P [\phi_r - (L_d - L_q) i_d] i_q \quad (8)$$

Where v_d , v_q , i_d and i_q are the respective voltage and current components in d-q-axes while E_d and E_q are the d-q-axes back-emf components and T_e is the electro-magnetic torque experienced by the generator. L_d , L_q and r_s are the stator leakage reactances and winding resistance while ϕ_r and P is the constant rotor flux and the number of pole-pair of the PMSG, respectively, whose rated power is 90 KW. The instantaneous disturbances in the rotor torque and shaft speed which follows from wind speed variations and shaft dynamics as in are directly reflected in the output voltage and power of the generator. The amount of ripples in the dc side voltage after rectification of the PMSG ac voltage decides the value of the dc bus line inductor which is responsible for suppressing the ripples

B. Battery Energy Storage System

Lithium-ion battery is used for transient power support at the dc link for stabilization of V_{dc} , because of high power density and capability of undergoing higher charging/discharging states without degradation of its life unlike cheaper lead-acid batteries. Due to such properties in spite of its high cost these batteries are suited for wind based hybrid power systems and electric vehicles. The battery terminal voltage is a combination of constant, polarization and exponential components as given in (11) [1, 3] and can be modeled based on its charging/discharging dynamics.

$$V_b = V_c - A_p \frac{C_q}{C-q} - R_{ib} + K e^{-iq} \quad (11)$$

$$Q = (1 - SOC_i) C + \int i_b dt \quad (12)$$

III. FMEA OF THE HYBRID SYSTEM AND POSSIBLE METHODS OF FAULT MITIGATION

FMEA is done on the system to find the chance or probability of failure of different system components. This is a reliability analysis of the system which depends on the regular inspection, monitoring and expert knowledge of the system components which are prone to failures and may affect the performance of the system severely. FMEA is used to structure mitigation for risk reduction based on either failure effect severity reduction or on lowering the probability of failure or both [4, 5]. Particularly the power converters in the proposed system may be prone to open circuit or short-circuit faults due to excessive heating of the devices. The temperature of the components depends upon the magnitude of the active current it handles and instantaneous voltage build up across switches [6, 7]. Apart from the converters the line inductors and the shunt capacitors may fail due to very high increase in the rate of current and voltage experienced by the device, respectively.

The root cause behind these failures is not only the continuous heating effect but also the rate of rise in temperature and development of hot spots due to inefficient distribution of heat and also improper cooling of the converters. Further with an increase in power densities of converters, available surface area for heat dissipation decreases. For this reason the converters are generally derated under normal operation which increases reliability but does not increase component cost significantly. Different failure modes in the power converters of the proposed system are given in Fig. 2 along with their possible mitigation methods. As all the converters are connected directly to the dc link capacitor, a fault in any of the switches alters the dc link voltage and affects smooth power transmission. In case of short circuit fault across any switch, the dc link capacitor tends to discharge immediately delivering high fault current which may damage other switches in the converter leg or line inductors connected for ripple reduction. Hence immediate disconnection of the faulty converter from the remaining system is to be done after detection of high rate of increase in current and equals to fault current level. Under open circuit fault for the dc-dc converters of WECS, LCPV generator and BESS, MPPT from the renewable sources fails, and the dc link voltage will exactly follow the variations of wind speed and solar irradiance. It results in lowering of system efficiency, voltage stress on buck-boost converter for BESS and degradation in active power dispatch across the inverter. Retuning of integral gain of BESS voltage regulator may improve the dc link voltage stabilization. This alters the battery current reference within its permissible bias.

This performance may be improved with a ANFIS voltage control. Open circuit fault of the BESS

converter results in unidirectional and uncontrolled power compensation in the dc link. With open circuit fault in the uncontrolled rectifier of WECS, voltage imbalance will result at the ac side due to unidirectional power flow through the freewheeling diodes. For this rectifier the whole dc link voltage is experienced by a single diode of the converter leg and may fail. Therefore prolonged operation is not suggested after detection of open circuit faults. Though under sinusoidal PWM inverter drive system both voltage and current will remain balanced but it will result in dc offset current through the switches which degrades the output current quality [8]. Therefore the PI regulators for the d-q axes current may be returned to improve output current quality. Prolong operation with open circuit may cause over-current in the healthy switch of the same leg when turned on and will experience the full dc link voltage when turned off. Therefore isolation of the inverter from the dc link or ceasing its gate drive signals for all six switches may be required.

Fault Location	Nature of Fault	Mitigation Method
Faults in boost chopper and uncontrolled rectifier	Open Circuit Fault	Retuning of voltage regulator of the BESS
	Short Circuit fault	Isolation of the DC component from the remaining system
Faults in the bidirectional dc converter for BESS	Open Circuit Fault	Retuning of inverter voltage regulator for new d-axis current reference
	Short Circuit fault	Isolation of the battery bank from the dc link
Faults in the inverter	Open Circuit Fault	Resetting of gain values for inverter current regulators
	Short Circuit fault	Isolation of the inverter from the dc link

Fig. 2 Faults in converter switches and their possible mitigation

As short circuit failures are more frequent in converters, detection of sudden high rate of rise in the device current and when it equals fault current level urges opening of the faulty dc converter/rectifier connecting it to the dc link or cease of gate drive signal for the inverter. The suggested control for disconnection is shown in Fig. 3 for the LCPV generator and the battery, where the isolator Sw1 is Normally Closed (NC) but is opened when the time rate of rise of the inductor current (di/dt) exceeds its maximum limit 'k'. Soft isolation of the PMSG generator isolates the WECS for a short circuit in either the boost chopper or the uncontrolled rectifier

IV. DESIGN OF ADAPTIVE NEURO-FUZZY CONTROLLER

Adaptive Neuro Fuzzy Inference sSystem (ANFIS) integrates the best features of fuzzy systems and neural networks, and it has potential to capture the benefits of both in a single frame work. ANFIS is a

kind of artificial neural network that is based on Takagi-sugeno fuzzy inference system, which is having one input and one output. Using a given data set, the toolbox function of ANFIS constructs a Fuzzy Inference System (FIS) where as the membership function parameters are tuned (adjusted) using a back propagation algorithm. In order to have an idea of optimized ANFIS architecture for proposed control, an initial data is generated from normal PI regulator and the data is saved in workspace of MATLAB. Then the ANFIS command window is opened by typing ANFIS editor in the main MATLAB window. Then the data previously saved in workspace is loaded in the ANFIS command window to generate an optimized ANFIS architecture as shown in Fig.3.

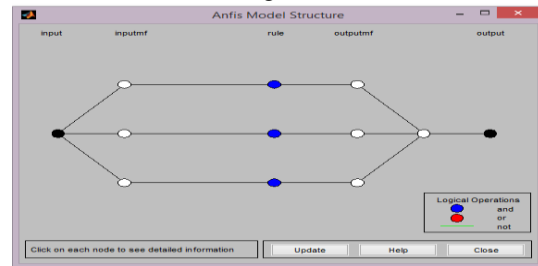


Figure. 3 Optimized ANFIS architecture suggested by MATLAB/anfis editor.

Is shown In Fig.4 The proposed ANFIS based control architecture. The node functions of each layer in the ANFIS architecture are described as follows:

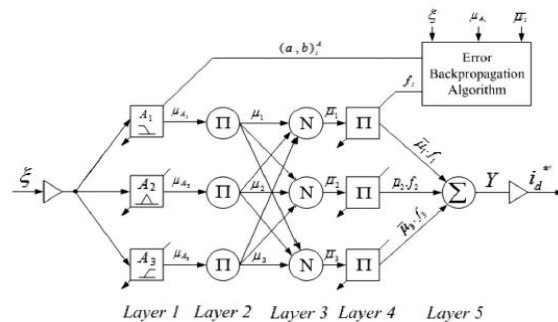


Figure. 4 Schematic of the proposed ANFIS-based control architecture.

The error between reference dc-link voltage and actual dc-link voltage ($\xi = V_{dc}^* - V_{dc}$) is given to the neuro-fuzzy controller and the same error is used to tune the precondition and consequent parameters [10]. The control of dc-link voltage gives the active power current component (i_d^*), which is further modified to take in account of active current component injected from RES (i_{Ren}).The node functions of each layer in ANFIS architecture are as described below:

Layer 1: This layer is also known as fuzzification layer where each node is represented by square. Here, three membership functions are assigned to each input. The trapezoidal and triangular membership functions are used to reduce the computation burden as shown in Fig. 5. And the corresponding node equations are as given below:

$$\left. \begin{aligned} \mu_{A1}(\varepsilon) &= \begin{cases} 1 & \varepsilon \leq b_1 \\ \frac{\varepsilon - a_1}{b_1 - a_1} & b_1 < \varepsilon < a_1 \\ 0 & \varepsilon \geq a_1 \end{cases} \\ \mu_{A2}(\varepsilon) &= \begin{cases} 1 - \frac{\varepsilon - a_1}{0.5b_2} & |\varepsilon - a_2| \leq 0.5b_2 \\ 0 & |\varepsilon - a_2| \geq 0.5b_2 \end{cases} \\ \mu_{A3}(\varepsilon) &= \begin{cases} 0 & \varepsilon \leq a_3 \\ \frac{\varepsilon - a_1}{b_1 - a_1} & a_3 < \varepsilon < b_3 \\ 1 & \varepsilon \geq b_3 \end{cases} \end{aligned} \right\} \quad (12)$$

Where the value of parameters (a_i, b_i) changes with the change in error and accordingly generates the linguistic value of each membership function. Parameters in this layer are referred as premise parameters or precondition parameters.

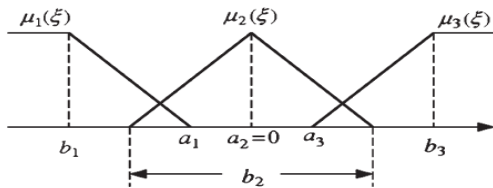


Figure. 5 Fuzzy membership functions.

Layer 2: Every node in this layer is a circle labeled as Π . which multiplies the incoming signals and forwards it to next layer

$\mu_i = \mu_{Ai}(\varepsilon_1) \cdot \mu_{Bi}(\varepsilon_2) \dots i=1,2,3,\dots$ But in our case there is only one input, so this layer can be ignored and the 5w output of first layer will directly pass to the third layer. Here, the output of each node represents the firing strength of a rule.

Layer 3: Every node in this layer is represented as circle. This layer calculates the normalized firing strength of each rule as given below:

$$\bar{\mu}_i = \frac{\mu_i}{\mu_1 + \mu_2 + \mu_3} \quad (13)$$

Layer 4: Every node in this layer is a node function

$$O_i = \bar{\mu}_i \cdot f_i = \bar{\mu}_i (a_0^i + a_1^i \varepsilon) \quad i=1,2,3.$$

where the parameters (a_0^i, a_1^i) are tuned as the function of input (ξ). The parameters in this layer are also referred as consequent parameters.

Layer 5: This layer is also called output layer which computes the output as given below: The output from this layer is multiplied with the normalizing factor to obtain the active power current component

V. SIMULATED RESULTS AND DISCUSSIONS

As per IEC 61400-2, blade pitch control for limiting extraction of power from wind turbine is essential when the generated power exceeds the rated power of the turbine to avoid its overloading [9]. The required pitch angle, β is generated from the power difference of turbine rated power and actual power. Fig. 4b shows the blade pitch angle control where the power error, ΔP , is sent to a PI regulator that generates the reference pitch angle. When $\Delta P < 0$, the limiter restricts the pitch angle reference to zero but when $\Delta P > 0$, the pitch actuator actuates the necessary pitch angle change of the blades to limit the extracted power. The dynamics of the pitch angle actuator is non-linear and depends upon saturation limits on pitch angle and pitch rate.

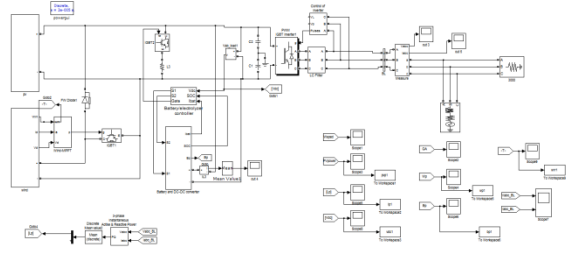


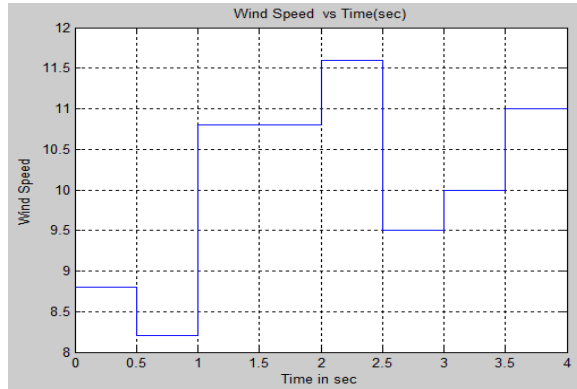
Fig 6 MATLAB/SIMULINK Model of the Proposed PV-Wind Hybrid Systems

The power transfer efficiency of a LCPV is about 25%, hence focus should be given on maximum extraction from such generator unconditionally in a grid connected system as any surplus power dispatched by the inverter will get consumed at the grid which behaves as a virtual load. Deviations of V_{dc} are corrected by optimum power extracted from WECS and the control of the BESS. The boost voltage fed at the common dc bus by the LCPV generator is as per (1).

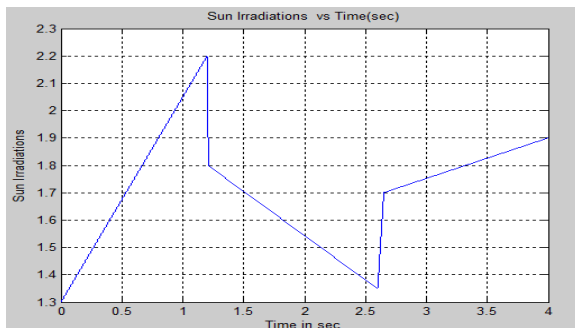
$$V_{boost} = \frac{1}{1-d} \{V_{pv} - I_L(R_s + L_s)\} \quad (15)$$

where d, I_L and (R_s, L_s) are the duty cycle of the chopper, solar generator load current and parameters of the boost converter, respectively. A basic hill-climb approach is used for tracking maximum power operating point where the control inputs

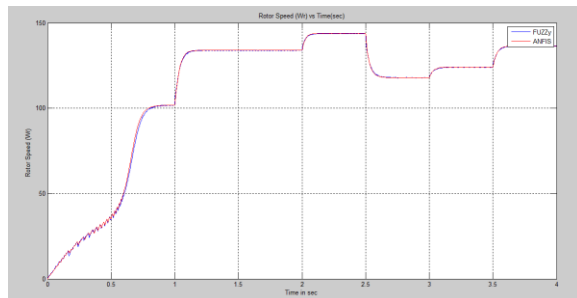
considered are dP_{pv}/dV_{pv} and its rate of change [10] and change in duty-cycle as the output. Mamdani type ANFIS control with five triangular membership functions for the two inputs Error (E) and Change in Error (CE) and the output which is perturbation in d are considered with its rule matrix given in Table 4. Input membership functions are considered tilted towards centre as maximum occurrences of errors are around the '0' crisp value.



(a)

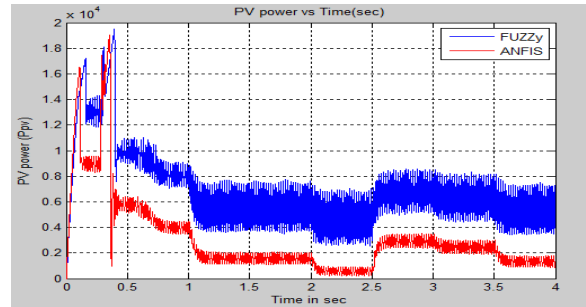


(b)

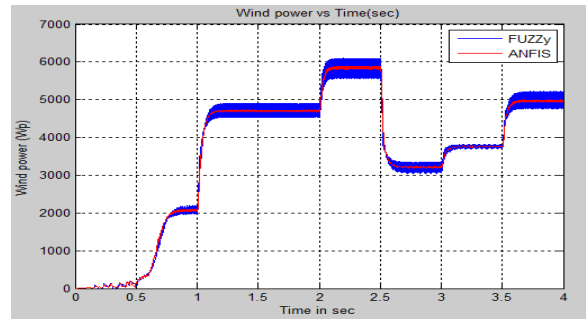


(c)

Fig. 7 Input characteristics of wind turbine and LCPV generator (a) Wind speed (b) Solar irradiance for LCPV (c) Rotor Speed



(a)



(b)

Fig. 8 Power management and error tracking for different modes of operation (a) Solar Power (b) Wind Power

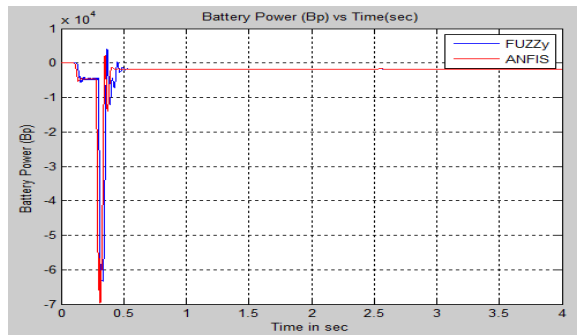
With the considered input source variations, ANFIS controllers help to track the correct instantaneous operating points for all controllers. Furthermore, performances of the two inverter current control techniques have proven that the ANFIS PD+I control provide better time domain response than the classical PI control. The wind speed profile considered here is given in Fig. 6(a).

Operation by mode 2 although produces almost similar oscillations in system responses but yields lesser power at the inverter output so onwards responses with this method is not shown. The active power management at the inverter output and dc power extracted from the wind generator for mode 1 and mode 3, respectively, are shown in Figs. 9(a) and (b). Fig. 9(a) shows active power dispatched by mode 3 is higher particularly after 2.5 s as compared with Fig. 7 for mode 1. Thus grid support is also higher in mode 3 reducing its active power burden of the local load. Power extraction from WECS again is also higher by mode 3 as shown in Fig 7 particularly after 2.5 s. The dc link voltage shown in Fig. 9(d) indicates mode 3 has lesser undershoot and oscillations of the dc link voltage about its reference value compared with mode 1. The grid inverter is supposed to compensate for the instantaneous load reactive power to improve load power factor and to control voltage droop at the inverter output. Fig.8 shows the compensation done by mode 3

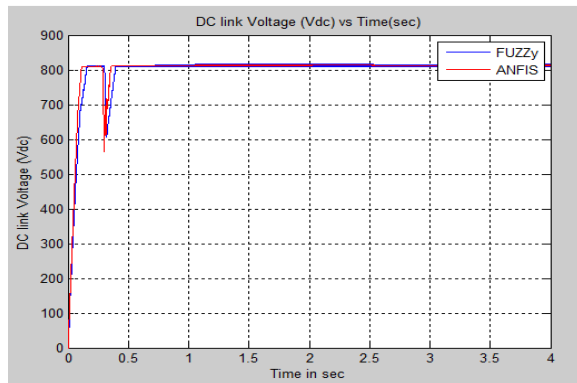
tracks the load requirement much closely with lesser oscillations than that mode 1. Figs. 8 (a) and (b) show the difference in the two modes in reactive power compensation at the PCC. While Fig. 8(a) shows a much improved stability for the compensation by mode 3 resulting in average grid reactive power requirement to zero, Fig. 8(b) gives a picture of poor stability by mode 1 with much higher oscillations. A comparison of load reactive power compensation as shown in Fig. 8(c) gives precise difference in the stability performances of the two modes.



(a)



(b)

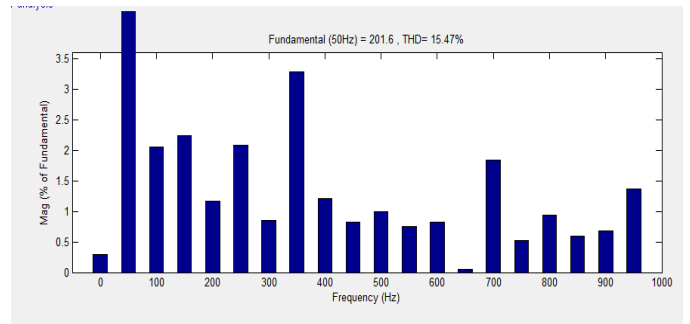


(c)

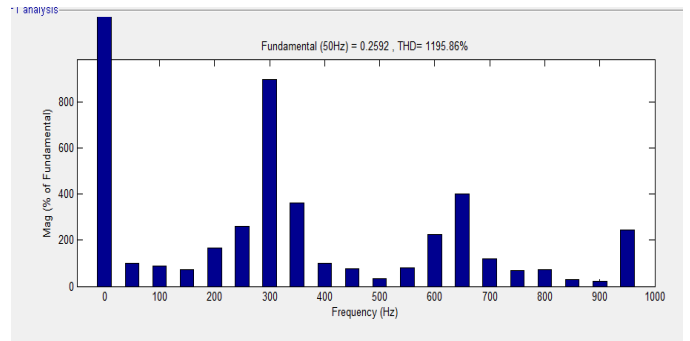
Fig. 9 Active power management by OPPT-ANFIS and MPPT modes (a) Active powers at the PCC by OPPT-ANFIS mode (b) Active powers at battery (c) DC link voltage

VI. BIDIRECTIONAL POWER FLOW CONTROL FOR BESS

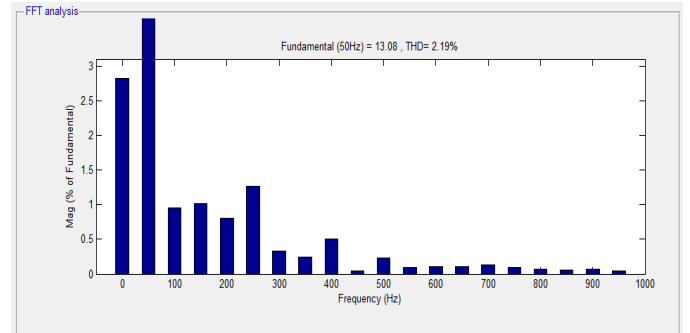
With a transient power mismatch between the generated and the consumed, V_{dc} deviates from its reference value, zero, which hampers smooth power transfer at the inverter output, de-stabilizing the output frequency from its nominal value [2, 11]. BESS controls the power flow at the common dc link stabilizing V_{dc} at its reference value V_{dc} ref. A dc buck-boost converter with IGBT switching is used for the model. The dynamics of the common dc link capacitor which controls battery current



(a)



(b)



(c)

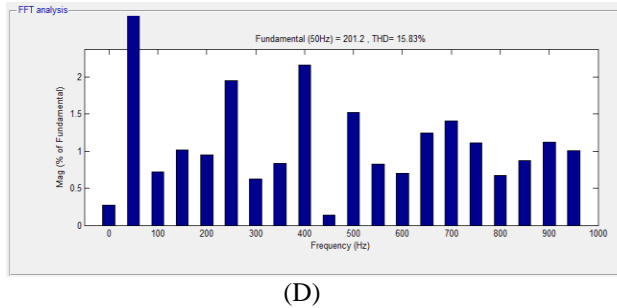


Fig. 10 THD of inverter voltage and current for MPPT and OPPT-fuzzy modes of operation (a) Voltage THD for

FUZZY mode (b) Voltage THD for FUZZY mode (c) Current THD for ANFIS mode (d) Current THD for ANFIS mode

INVERTER VOLTAGE AND CURRENT QUALITY IN TERMS OF THD

THD inverter	Modes of operation		
	FUZZY	ANFIS	FUZZY-ANFIS
Voltage	1195.86%	15.83%	1211.69%
Current	15.47%	2.19%	17.66%

VII.CONCLUSION

This work emphasises to extract maximum power from the 2.2X concentration LCPV solar generator and optimum power from a PMSG based direct driven wind power generator to provide necessary power to the local load and the grid. The power extractions are done intelligently using ANFIS control but wind power being the dominant contributor amongst the two, inject high frequency oscillations in the dc link power. Therefore extraction of power from this generator by the proposed method focuses to stabilize the dc link voltage and reduce active power mismatch at the inverter output. This method utilizes intelligently the knowledge of transient power imbalance at the dc link and the variation of load current to extract and dispatch maximum possible power with an improved quality at the inverter output. The system functions in grid supporting mode by dispatching the active power generated and reactive power compensation of the load wholly. Frequency and magnitude of the inverter output voltage is maintained at its desired nominal value without any voltage sags/swells as load changes. Anfis PD+I control of the inverter proves to be the best amongst the three modes of operation discussed in stabilizing dc link voltage, battery power control, improved grid support and improving THD of the inverter output voltage and

current. FMEA of the power conditioning system is done and possible mitigational methods are suggested for a ride-through of the system in the event of faults. The proposed control method under steady natural resources may produce marginal improvement as compared with the performances of the classical control.

REFERENCES

- [1] Hajizadeh, A., Tesfahunegn, S., Undeland, T.: ‘Intelligent control of hybrid photo-voltaic/fuell cell/ energy storage generation system’, J. Renew. Sust. Energy-AIP, 2011, 3, (4), pp. 1–17
- [2] Uehara, A., Pratap, A., Goya, T., et al.: ‘A coordinated control method to smooth wind power fluctuations of a PMSG-based WECS’, IEEE Trans Energy Convers., 2011, 26, (2), pp. 550–558
- [3] Wang, B., Rogers, C., Peng, F., et al.: ‘Energy storage system based power control for grid-connected wind farm’, IJEPES, 2013, 44, pp. 115–12
- [4] Ribeiro, E., Cardoso, A., Boccaletti, C.: ‘Open circuit fault diagnosis in interleaved DC–DC converters’, IEEE Trans. Power Electron., 2014, 29, (6), pp. 3091–3102
- [5] Kahrobaee, S., Asgarpoor, S.: ‘Risk-based failure mode and effect analysis for wind turbines (RB-FMEA)’. NAPS, 2011
- [6] Sheng, H., Wang, F., Tipton IV, C.W., et al.: ‘A fault detection and protection scheme for three-level DC–DC converters based on monitoring flying capacitor voltage’, IEEE Trans. Power Electron., 2012, 27, (2), pp. 685–697
- [7] Jlassi, I., Estima, J. D., Khil, S. KEI., et al.: ‘Multiple open-circuit fault diagnosis in back-to-back converters of PMSG drives for wind turbine systems’, IEEE Trans. Power Electron., 2015, 30, (5), pp. 2689–2702
- [8] Kastha, D., Bose, B.: ‘Investigation of fault modes of voltage-fed inverter system for induction motor drives’, IEEE Trans. Ind. Appl., 1994, 30, (4), pp. 1028–1038
- [9] Kurahane, K., Senjyu, T.A., Yong, A., et al.: ‘A hybrid smart AC/DC power system’, IEEE Trans Smart Grid, 2010, 1, (2), pp. 199–204
- [10] Larbes, C., Cheik, S., Obeidi, T., et al.: ‘Genetic algorithms optimized fuzzy logic control for maximum power point tracking in photovoltaic system’, J. Renew. Energy, 2009, 34, pp. 2093–2100
- [11] Chen, Y., Chen, C., Wu, H.: ‘Grid-connected hybrid PV/wind power generation system with improved dc bus voltage regulation strategy’. Power and Electronic Conf., APEC, 2006